

This article was downloaded by:

On: 14 January 2011

Access details: *Access Details: Free Access*

Publisher *Taylor & Francis*

Informa Ltd Registered in England and Wales Registered Number: 1072954 Registered office: Mortimer House, 37-41 Mortimer Street, London W1T 3JH, UK



## **Molecular Simulation**

Publication details, including instructions for authors and subscription information:

<http://www.informaworld.com/smpp/title~content=t713644482>

## **An Atomic-Scale Simulation of Lubricated Motion**

J. Corish<sup>a</sup>; D. A. Morton-Blake<sup>a</sup>

<sup>a</sup> Chemistry Dept., Trinity College, Dublin 2, Ireland

**To cite this Article** Corish, J. and Morton-Blake, D. A.(1998) 'An Atomic-Scale Simulation of Lubricated Motion', *Molecular Simulation*, 21: 1, 41 – 66

**To link to this Article:** DOI: 10.1080/08927029808022049

**URL:** <http://dx.doi.org/10.1080/08927029808022049>

PLEASE SCROLL DOWN FOR ARTICLE

Full terms and conditions of use: <http://www.informaworld.com/terms-and-conditions-of-access.pdf>

This article may be used for research, teaching and private study purposes. Any substantial or systematic reproduction, re-distribution, re-selling, loan or sub-licensing, systematic supply or distribution in any form to anyone is expressly forbidden.

The publisher does not give any warranty express or implied or make any representation that the contents will be complete or accurate or up to date. The accuracy of any instructions, formulae and drug doses should be independently verified with primary sources. The publisher shall not be liable for any loss, actions, claims, proceedings, demand or costs or damages whatsoever or howsoever caused arising directly or indirectly in connection with or arising out of the use of this material.

# AN ATOMIC-SCALE SIMULATION OF LUBRICATED MOTION

J. CORISH and D. A. MORTON-BLAKE \*

*Chemistry Dept., Trinity College, Dublin 2, Ireland*

*(Received January 1998; accepted March 1998)*

Alkyl chain monolayers and bilayers are investigated by static atomistic simulation. Optimisation of the chain conformations by imposing sets of random torsions leads mainly to all-*trans* structures. The relaxations of *Y*-configuration bilayers are investigated after imposing mutual displacements to the interface. Energy profiles for sliding motions of the bilayer show periodic behaviour from which the friction associated with the motion is related to the maximum force in each cycle of the profile. This is consistent with the observation that the lubricating action of an alkyl chain increases with the length of the chain. Derived shear strength values are reasonably close to experimental measurement. For small displacement intervals the profiles showed sharp energy spikes that are analogous to the 'stick-slip' discontinuities found in low-speed surface force studies of molecular layers. These are discussed in terms of low-lying metastable states from which, on further displacement, the system relaxes to the ground state.

**Keywords:** Nanoscale; atomistic simulation; alkyl-chain bilayers; bilayer displacement; lubrication

## 1. INTRODUCTION

The interaction between alkyl chains plays an essential rôle in the forces within and between amphiphilic monolayers. The latter constitute the basis of that form of matter that includes surfactants, micelles, Langmuir-Blodgett (LB) films and lipid bilayers. These are built up of flexible chains consisting of a polar 'head', such as a carboxylic acid group, and an aliphatic 'tail' which is often a long alkyl group [1] although links other than C—C may also be present provided they confer flexibility on the chain.

---

\*Corresponding author.

A third component occurring in an LB film is the substrate which is usually the surface of a polar liquid, but may also be a solid such as glass.

When monolayers come together to form a multilayer film the components may show various mutual configurations; the one occurring in a given film depends on the nature of the head, the tail and the substrate. A common configuration found in films and lipid membranes is the 'Y-structure' in which the monomers interface head-to-head and tail-to-tail. The tail-to-tail interactions are of particular interest in the atomic-level description of the mechanism of lubrication and in the structure of a lipid bilayer. It is generally accepted that long-chain fatty acids adhere to the substrate through their polar heads, leaving the hydrocarbon tails in the multilayer to enmesh or interact. Although the overall thickness of the layers is small in comparison with the asperities in engineering contact surfaces it has been established that the Y-structure is important in the mechanism of surface lubrication [2, 3]. Even in bulk samples it has been known for several decades that the friction of surfaces lubricated with long-chain fatty acids or alkanes decreases with the length of the chain [4]. In the present work we suppose that the trends and phenomena that have been observed from experiment have an atomic origin and we shall attempt explanations of these effects using the results of our atomistic simulation investigations.

The development of recent sensitive techniques to measure surface forces has introduced a novel dimension to the investigation of the interaction between surfaces. Chugg and Chaudhri have measured tribological parameters for the sliding of alkyl-tailed surfactant layers deposited on solids in layers as thin as a monolayer [5]. The frictional forces incurred by a metal tip sliding on a graphitic basal plane have been measured by atomic force microscopy [6]. Using a piezoelectric tube to monitor the forces and an optical device to measure displacements, Israelachvili and his coworkers have detected the response of liquid-state molecules to the sliding motion of their confining solid surfaces [7–10]. In this way the latter investigators have elucidated the behaviour, on a microscopic scale, of globular and chain molecules acting as lubricants between the moving surfaces [11]. The response of the molecular layers is monitored by the forces whose profile depends on the conditions imposed on the system such as normal load and sliding velocity. The authors found force profiles that were periodic in time, exhibiting a zig-zag variation or 'stick-slip' which were interpreted as an alternating sequence of local freezing and melting processes caused by the shearing of the layers in the contact region which in turn ruptures and re-forms their local order [12].

The implications of these results on the atomic scale of the lubricant molecules have seeded various simulation studies of the systems, mainly by Molecular Dynamics and Monte Carlo methods [12–20] using large cells or simulation boxes that confer high degrees of freedom on the chain segments as they evolve towards equilibrium, using pseudo-atoms to represent non-bonded interactions for methylene and methyl groups. The intention of the present work is to examine whether the effects observed by these and other methods can be given an alternative description by a model in which all the atoms in the sliding system considered are included explicitly, and in which details of their motions are sought by performing static lattice calculations.

## 2. METHOD OF CALCULATION

This work describes the static atomistic simulation of the enmeshing of the aliphatic chains in such a bilayer-type system. The latter is represented by the alkyl tails only, the function of the heads being recognised by simply anchoring the chains at their ends on to formal atoms labelled  $C_{(0)}$  which occupy hexagonal sites on a plane. The positions of these sites are such that the whole system generates a two-dimensional lattice. Various types of mutual displacements will be imposed on the monolayers in order to model the changing interactions of the alkyl chains involved in the considered motions.

The lattice energy is calculated atomistically by the application of non-bonded atom-pair ‘potentials’ (energy functions) for C and H atoms to a proposed unit cell with periodic boundary conditions. The potentials selected are the set generally known as the Williams IV [21]

$$V_{CC}(r) = 3626.626 \exp(-r/0.2778) - 24.6367 r^{-6} \quad (1)$$

$$V_{HH}(r) = 115.116 \exp(-r/0.2674) - 1.1844 r^{-6} \quad (2)$$

$$V_{CH}(r) = 380.139 \exp(-r/0.2725) - 5.4206 r^{-6} \quad (3)$$

where  $V_{AB}(r)$  is the interaction energy contribution in eV for the atom pair  $(A, B)$  and where the interatomic distance  $r$  between  $A$  and  $B$  is in Ångströms ( $10^{-10}$  m). This set of potential functions leads to lattice structures of hydrocarbon lattices, particularly alkane chains, which are in good agreement with the results of diffraction investigations [22] and were

used in our investigation of alkyl-chain interactions in poly(3-alkylthiophenes) [23–25]. Since the bonds are assumed to be rigid no bond-stretching or bond-bending potentials are invoked in this work.

In earlier work we considered interactions between alkyl chains in the thermochromic polymer material poly(3-alkylthiophene) [23–25], which are disposed in a configuration which is similar to that in the bilayer system described here. For structures close to those of ambient pressure conditions the chain configurations were optimised by Hessian matrix methods, which use the curvature of the energy function in coordinate space to minimise the energy. Although long flexible chains have a large number of energy minima, it was comparatively easy to probe wells near those associated with the fully-extended configuration and thereby show that the latter structure corresponded to the lowest energy [23]. Under higher pressure conditions, however, where the interdigitation of adjacent alkyl chains results in a less ordered structure, the location of the global energy well becomes a difficult task. We therefore supplemented the Hessian matrix approach to the energetics of chain torsions around alkyl C—C bonds by a method that relaxes the conformations by a series of random torsional angles [25].

A similar procedure is followed in the present work. In each defined bilayer configuration random torsions are applied to all seven C—C bonds in each alkyl chain (the six C—C bonds in hexyl plus that connecting the chain to the anchor atom C<sub>(0)</sub>). The system is considered to have relaxed when the application of one thousand trial torsions produces no lower energy. The resulting chain conformations are then analysed for useful structural parameters.

### 3. OPTIMISATION OF THE MONOLAYER STRUCTURE

No well-established structures have been proposed for the alkyl bilayers that are found in lubricated surfaces. In LB layers there is evidence of an approximately hexagonal two-dimensional lattice [26] and although the point-group symmetry of the structure lacks a C<sub>6</sub> axis we have used a pseudo-hexagonal cell in the present simulations (Fig. 1). Taking various values of the cell parameter  $d$  we optimised the angle between the carbon plane and the cell axis, which showed that the favoured angles for all  $d$  values were those producing a layer structure. (In the hexagonal lattice this implies chain setting angles of 0°, 60°, 120° *etc.*)

Figure 2 shows the changes in both the lattice energy and the root mean square of the torsional angles of the C—C bonds  $\varphi_{\text{rms}}$  (measured from the

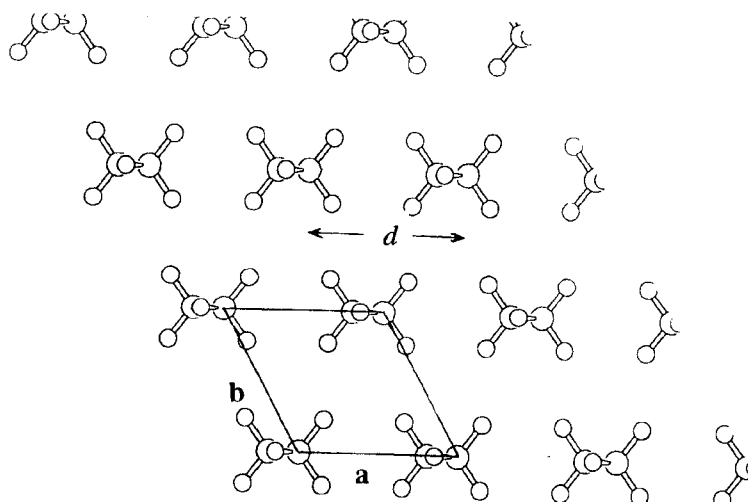


FIGURE 1 The two-dimensional lattice of alkyl chains modelling a Langmuir monolayer, viewed along the chain directions from the terminal methyl group. The lattice parameter  $d$  separates the chains along the pseudo-hexagonal axes  $a$  and  $b$ .

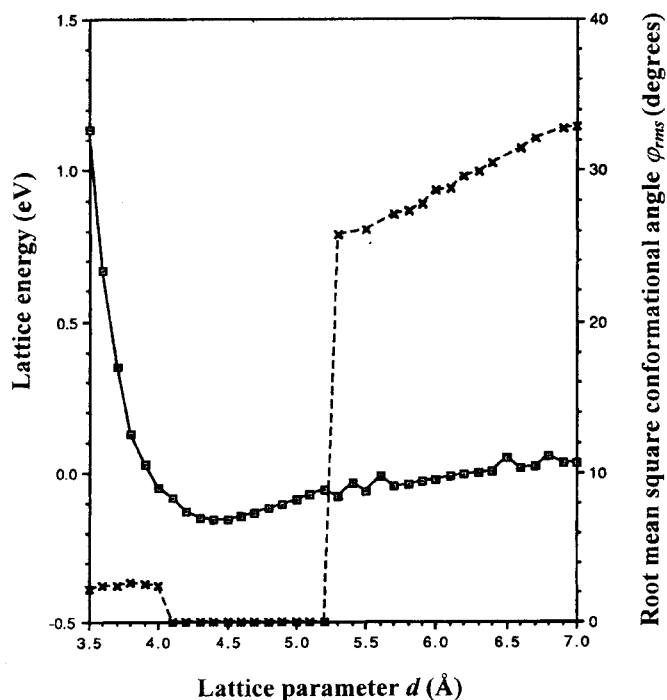


FIGURE 2 The lattice energy ( $-\square-$ ) and root mean square torsion angle  $\phi_{rms}$  in the C—C linkages ( $-\times-$ ) as a function of the chain separation parameter  $d$  defined in Figure 1.

*trans* conformation at  $0^\circ$ ) as the distance  $d$  between the chains is reduced. The computed energy in this and in the subsequent profiles measures just the conformation-dependent contribution to the lattice energy, which in our fixed-geometry approximation is the non-bonding interaction of atom pairs. Thus only energy *differences* will be physically useful in discussing the lattice energies. There is a well-defined energy well at  $d = 4.42 \text{ \AA}$ , corresponding to a mean molecular area of  $0.17 \text{ nm}^2$ . Values of this quantity measured in the condensed phases of alkyl-chain LB monolayers [27] are around  $0.19 \text{ nm}^2$ , but interestingly the  $0.17 \text{ nm}^2$  value is precisely that to which Glosli and McClelland's MD system optimised, in which they represented methylene and methyl non-bonded potentials by those for single 'pseudo-atoms' [16]. The curve, with its sharp rise in the energy as  $d$  is reduced from  $4.42 \text{ \AA}$  is reminiscent of the pressure-area isotherms measured for Langmuir monolayers [1]. While  $\varphi_{\text{rms}}$  is significantly different from zero when  $d$  exceeds the structural optimum value of  $4.42 \text{ \AA}$ , a diminishing chain separation clearly leads to increasing conformational order, resulting in a completely all-*trans* conformation at the minimum energy structure. Compressing the chains by further reduction of  $d$  results in a slight conformational disorder ( $\varphi_{\text{rms}} < 3^\circ$ ) probably arising from the particular orientations of the steric forces when the chains are in close contact.

The change from all-*trans* ( $\varphi_{\text{rms}} < 0^\circ$ ) at  $d > 5 \text{ \AA}$  results in chain conformations that are different from those at  $d < 4 \text{ \AA}$ . The torsional angles associated with the six C—C bonds (Fig. 3) show that in each chain the mean torsion  $\varphi_{\text{rms}} \approx 30^\circ$  is the result of large ( $> 60^\circ$ ) torsions around the  $C_{(0)}-C_{(1)}$  bonds linking the chains to the substrate, but much smaller values ( $< 20^\circ$ ) in the other bonds  $C_{(1)}-C_{(2)}$ ,  $C_{(2)}-C_{(3)}$  etc. As a result the chains almost retain their *trans* conformations, but tilt around the bonds linking them to the substrate. This result agrees with the observation of the  $33^\circ$  uniform tilt of the alkyl chains in monolayers of long-chain fatty acids on water at low lateral pressures ( $< 1 \text{ mN/m}$ ) while remaining all-*trans* [28].

## 4. THE BILAYERS

### 4.1. Mutual Penetration of the Layers

The enmeshing of two monolayers was investigated by placing the two monolayer lattices, each with the structure described in the previous section and with  $d = 4.42 \text{ \AA}$ , in a bilayer *Y* structure (tail to tail configuration) with a relative displacement of  $(\frac{1}{2}a, \frac{1}{2}a)$ . As shown in Figure 4 each alkyl chain

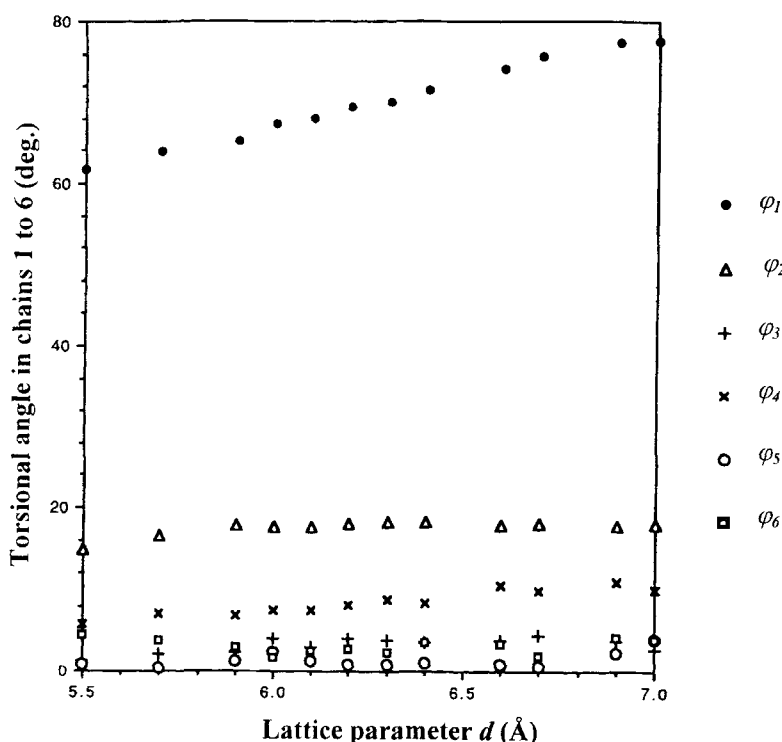


FIGURE 3 The torsional angles of the six C—C bonds in the hexyl chain monolayer in the  $d > 5.2$  Å régime of Figure 2. It shows that the chains remain almost *trans*, but tilt by twisting around the  $C_{(0)}-C_{(1)}$  bonds.

occupies a space over an inter-chain channel in the opposite layer. The parameter  $z$  measures the tip to tip separation of the chains. A positive  $z$  value describes a gap between the layers; a negative value corresponds to alkyl-chain interdigitation, or penetration of the monolayers.

It was found that, for a given separation  $z$ , the optimum procedure to ensure that the structure relaxes to the lowest, rather than a relative, minimum is to start from an already-relaxed structure whose  $z$  is fairly close to the one in question. (If however the  $z$  intervals are *too* close there is the possibility of accession to a train of metastable states leading to 'stick-slip' energy spikes, which will be discussed below. But we shall see that such a condition is evident from the profile and that allowance can be made for it). The procedure adopted in calculating the variation of the lattice energy as the layers penetrated was thus to allow the monolayers to approach in small  $z$  intervals, to energy-minimise and then to use the relaxed lattice as a



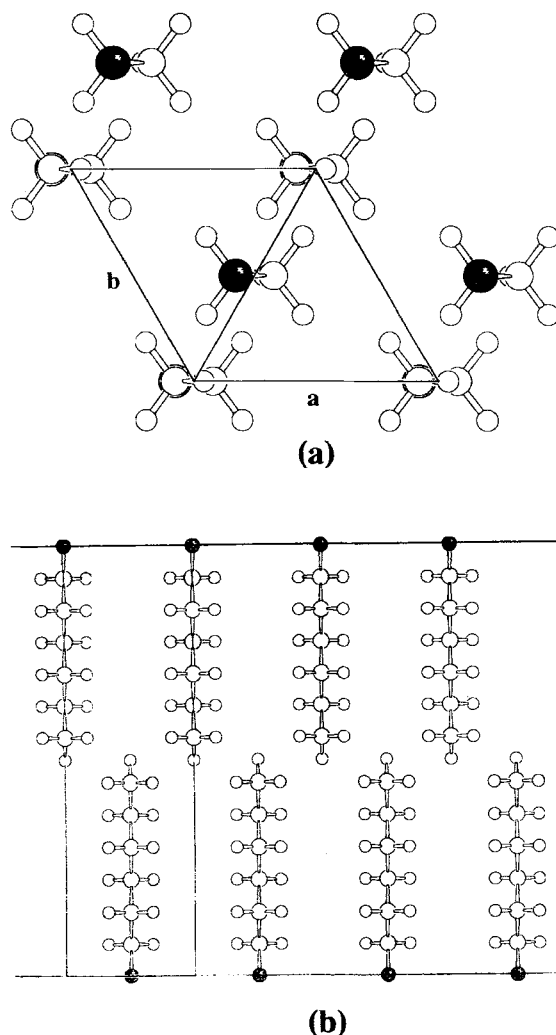


FIGURE 4 Model of the pseudo-hexagonal alkyl bilayer used in this work. The 'anchor' atom  $C_{(0)}$  is shaded in order to distinguish the chains in the two layers. The model is viewed (a) along the directions of the (initially all-*trans*) chains, and (b) along the *a* axis, normal to the chains. For clarity the structure is drawn with a chain separation  $d$  greater than its lowest-energy value.

starting point for the configuration corresponding to the next  $z$  value. Another reason for doing this was to avoid the problem of defining initial structures containing excessively short non-bonded atom separations. In such structures not only are the non-bonded atom-pair interaction energies uncertain at short atom-pair distances but the general form of the

Buckingham-type potential in Eqs. (1) to (3) becomes invalid at small  $r$  ( $< 0.9 \text{ \AA}$ ). Accidental jumps into this forbidden  $r$  range are minimised (usually precluded) by the procedure described, allowing all the interatomic separations remain in the energy-well range of the Buckingham functions.

The resulting profile in Figure 5 shows an energy which, overall, increases with greater mutual penetration of the layers. In order to ensure that the relaxation procedure had produced the lowest-energy lattice for each  $z$  value, calculations were conducted for several  $z$  ranges, the results of two of which, at  $z = 0.0$  and at  $z = +0.3 \text{ \AA}$ , are shown in Figure 5. Provided that the initial (maximum)  $z$  value was positive the profiles obtained were closely similar, and the two that are included in the Figure are the most disparate of

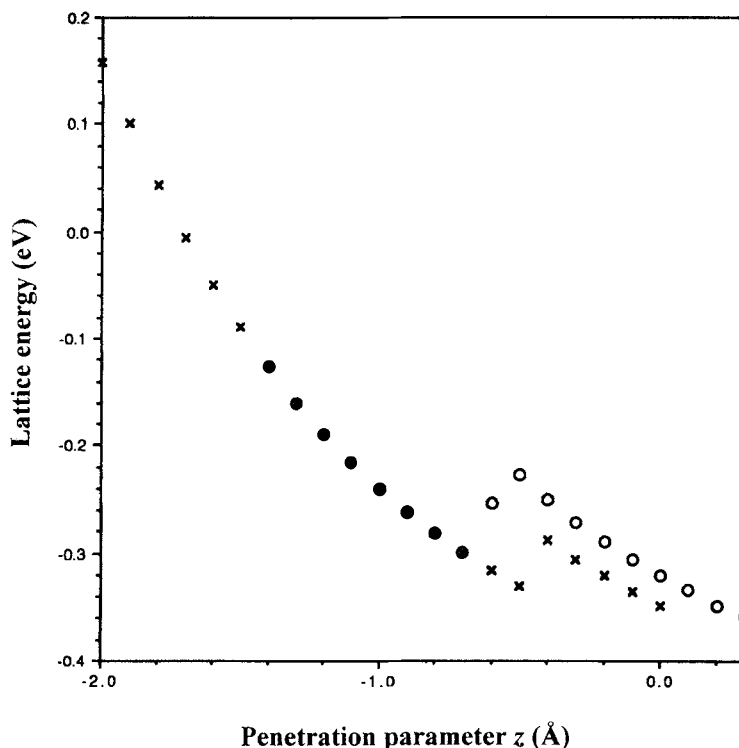


FIGURE 5 Two energy profiles for the mutual penetration of two hexyl monolayers starting from two different *initial* values of the penetration parameter  $z = 0.0 \text{ \AA}$  and  $z = +0.3 \text{ \AA}$  (plotted with symbols  $\circ$  and  $\times$  respectively). The parameter  $z$  measures the closest distance between the tips of the alkyl groups in the two monolayers; when positive it equals the gap between the layers and when it becomes negative it indicates the 'depth' to which the alkyl chains interdigitate.

these. On the other hand, when the relaxations were started from within the penetration region ( $z < 0$ ), the curves sometimes showed several discontinuities caused by the relaxation or settling of the chains into their lowest energy conformations. Such a feature appears in the two profiles in Figure 5. Despite several variations of the relaxation conditions (*e.g.*, initial starting position, random-number generation, maximum permitted jump of torsion-angle), the energy curves for the penetration of the layers always showed one or more settling-type discontinuities. This relaxation feature appears to be absent in the *separation* of the enmeshed layers; as  $z$  is increased from a negative value there are no discontinuities in the energy curve. The curves in Figure 6 show that the changes in the energy and chain conformation parameter  $\varphi_{\text{rms}}$  in the penetration/separation cycle are fairly reversible. With increasing penetration of the bilayer the departure of the alkyls from all-*trans* becomes more marked as they react to the strong inter-chain repulsions. In fact the acquisition of certain chain conformations by plasticised films upon imposition of a strain has been observed from infrared spectroscopy, and the authors discuss the consequent contribution of the additional conformation energy to the activation energy resulting from the strain [29].

#### 4.2. Lateral Displacement of the Layers

A mutual coplanar displacement corresponds to a 'sliding' of the monolayers, and is an attempt to simulate features in the motion of lubricated surfaces. Applying the energy calculation used in the previous section the energies of different lateral configurations of the monolayers were monitored by exploring the position of one of them in the  $xy$  plane at a chosen value of the layer separation  $z$ .

In view of (a) the uncertainties of the non-bonded interaction energies at small  $r$ , and (b) the fact that the method does not at present cater for distortions from standard molecular geometries, it was decided to avoid those layer configurations that would arise for extreme distortions of the chains. The investigations were thus confined to bilayer structures with penetrations  $|z|$  not greater than  $1.0 \text{ \AA}$ . The sliding motion within the bilayer was simulated by giving the layers a series of small displacements in their own planes. As was also found in the bilayer penetration motion described in Section 4.1, relaxation occurred most efficiently when the chain conformation at each stage of the 'slide' was taken to be the relaxed conformation of the immediately preceeding stage. The bilayer displacements were

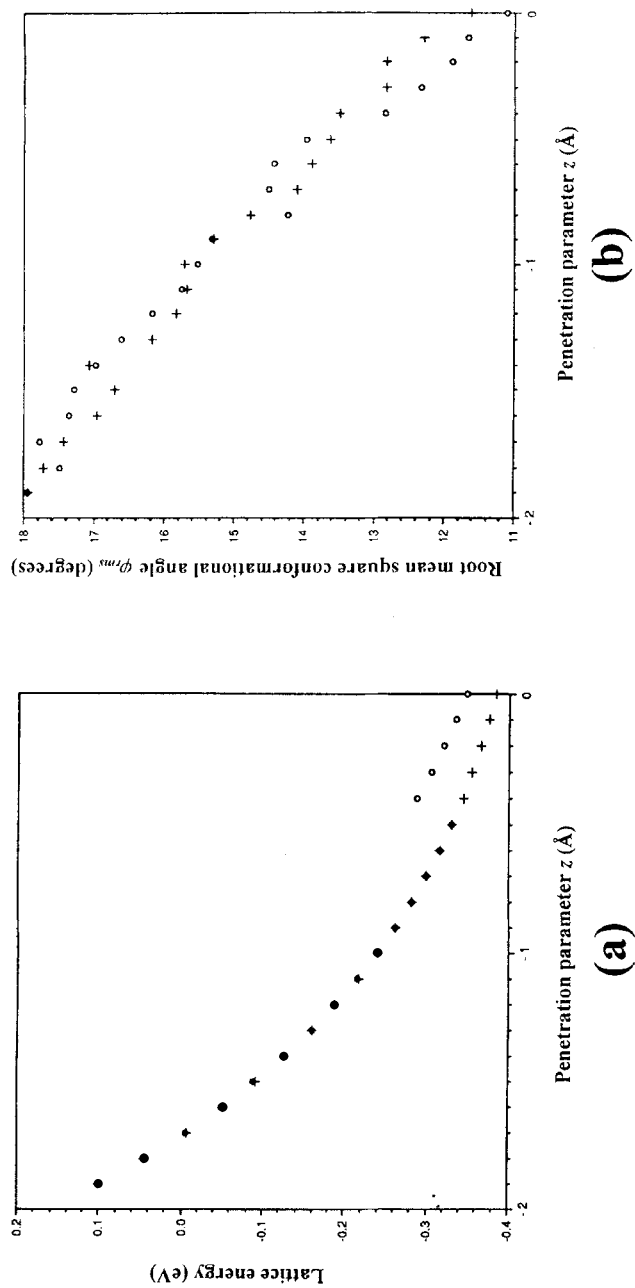


FIGURE 6 (a) The variation in energy when the hexyl bilayers of Figure 5 are (o) inserted into, and (+) withdrawn from, the enmeshed bilayer. The plots in (b) show the effect of these actions on the mean conformational angles of the alkyl chains in the system.

therefore taken at small intervals ( $0.2 \text{ \AA}$ ) along a direction in the plane of the moving layer.

We shall first discuss the results illustrated in Figure 7, showing the energy variation incurred when one layer slips over the other for a total displacement of  $10 \text{ \AA}$  in the  $a$  direction at a layer separation  $z = 0.0 \text{ \AA}$ . The figure includes data for two lengths of alkyl chain (hexyl  $\text{C}_6\text{H}_{13}$  and pentyl  $\text{C}_5\text{H}_{11}$ ). The zero layer-separation corresponds to a 'flush' condition for the methyl hydrogen atoms in each bilayer, *i.e.*, they are all on the same plane, but will be deflected as the layers are mutually displaced. The curves show higher energies for the shorter alkyl chain and demonstrate a periodicity that matches the spacing  $d = 4.42 \text{ \AA}$  along the  $a$  axis, with minima at  $x = 0, a, 2a, 3a, \dots$ , as might be expected from the relative positions of the layers shown in Figure 4(a). The profiles for both the hexyl

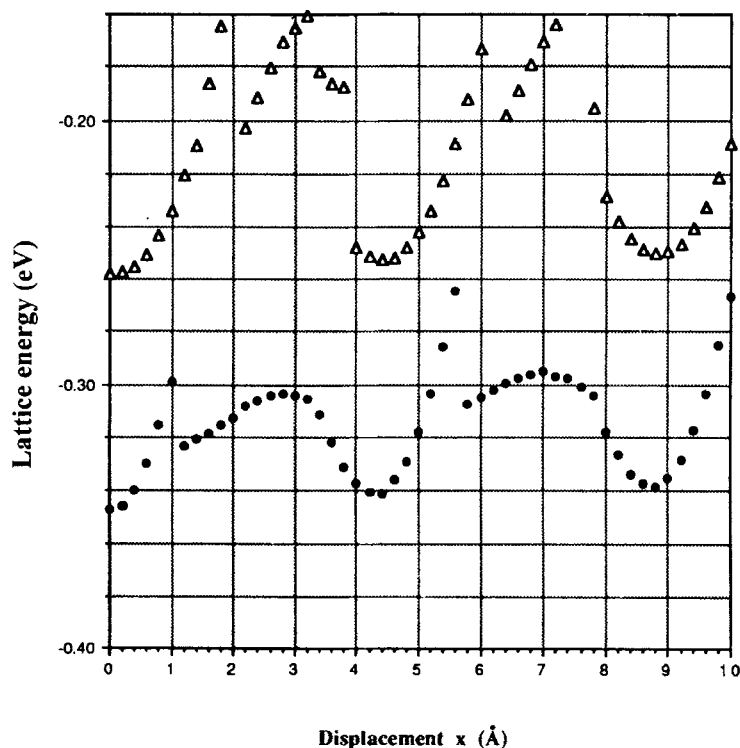


FIGURE 7 The energy profile for the mutual displacements along the  $a$  axis in the  $\text{C}_5\text{H}_{11}$  ( $\Delta$ ) and  $\text{C}_6\text{H}_{13}$  ( $\bullet$ ) bilayers at a tip-to-tip separation  $z = 0 \text{ \AA}$ . (In Figs. 7–8 grid lines are included to aid the estimation of the energy barriers.)

and the pentyl bilayers show discontinuities consisting of energy ‘spikes’. We attributed the corresponding discontinuities in the penetration profiles in Figure 5 to relaxation from local metastable lattice states to the ground state, and it is probable that the discontinuities in Figure 7 (which also result from a relative displacement of the layers) have a similar origin. This will constitute the subject of a discussion below. The energy profile also shows that while the sliding motion in hexyl involves an energy barrier of 0.04 eV the barriers in the shorter pentyl chain are about twice this value.

If the atomic origin of the frictional force operating in lubricated surfaces is a measure of the rheological forces between the moving layers, and if this resistance in turn depends on the energetics describing the layer displacements, then it should be possible to relate some of the features of our calculated energy profiles to observation. It was long ago observed that the frictional force between two contact surfaces that are lubricated with unbranched alkyl chain molecules (fatty acids and paraffins) has an approximate inverse variation with chain length [4]. The higher energy barrier which Figure 7 shows to be associated with the shorter chain would therefore appear to be consistent with this observation. In Figure 8 the **a** axis displacement of the layers which now penetrate to a depth of 0.5 Å give results which are consistent with the above as both the absolute energies and the energy barriers increase with diminishing chain length. The hexyl chain shows a barrier of just over 0.04 eV while pentyl has a substantially greater barrier of approximately 0.10 eV (unlike the hexyl profile the presence of stick-slip spikes for pentyl betrays the lack of complete relaxation at some mutual displacements, but the true height would appear to be between 0.08 and 0.12 eV). The barrier associated with the short butyl (C<sub>4</sub>H<sub>9</sub>) chain is still larger, perhaps as much as 0.14 eV.

For the reasons described at the beginning of Section 4.2 we limited our investigations mainly to those layer displacements which are not likely to lead to conditions of such strain that would cause deformations in bond lengths and bond angles. Nevertheless it is instructive to attempt simulations of frictional motion under higher energy (or pressure) conditions where the effect of *shearing* of the layers may occur due to the penetration of the alkyl-chain layers. The profiles in Figure 9 show a steady increase of the energy barrier when the layers slide along the direction of the **a** axis with progressively greater penetration of the layers ( $z = +0.5$  to  $-2.0$  Å), the effect being accompanied by more pronounced stick-slip spikes. If the layers were displaced in a direction normal to the **a** axis, the alkyl chains would be expected to encounter high energy barriers as one layer is dragged across the chains and channels that are aligned along the **a** axis.

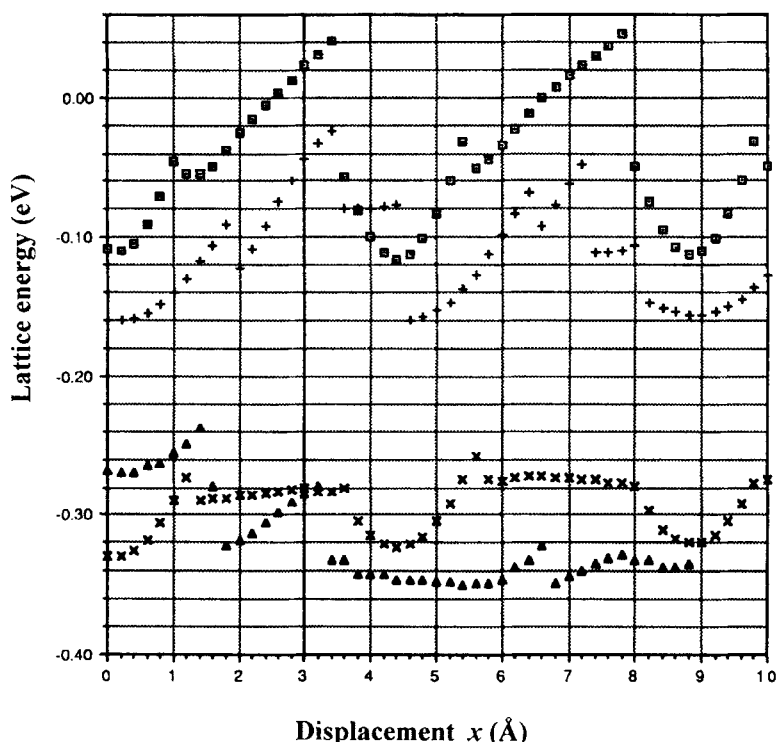


FIGURE 8 Energy profiles for  $a$ -axis displacements in  $C_4H_9$  ( $\square$ ),  $C_5H_{11}$  (+),  $C_6H_{13}$  ( $\Delta$ ) and  $C_8H_{17}$  ( $\times$ ) bilayers.

When the layers are displaced in the  $y$  direction, which is normal to the  $a$  axis and thus perpendicular to the grooves along  $a$  as seen in Figure 1, the adherence of the energy profile to the lattice periodicity diminishes with increasing penetration  $-z$  (Fig. 10). As might be expected for a condition in which the chains of one layer are dragged 'broadside on' across the chains and channels of the second layer, the stick-slip energy spikes are initially significantly higher than those for displacement along  $x$ . However the amplitudes of the energy peaks and wells rapidly become subject to a damping which diminishes the effective energy barriers. The demands for computing power to perform such calculations for displacements longer than the  $10\text{ \AA}$  limit considered here would necessitate impractically high computing times to demonstrate the shape of the energy profiles for distances of several nanometers but trial calculations indicate that the damping effect strongly suggested by the profiles in Figure 10 is continued with a steady reduction of the effective barriers.

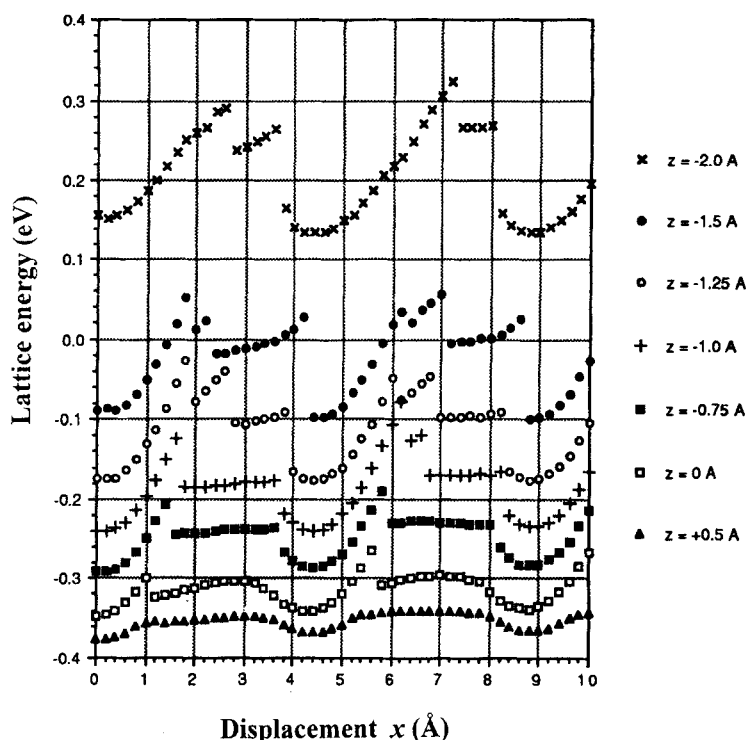


FIGURE 9 a-axis displacement profiles in  $C_6H_{13}$  at different values of the penetration parameters  $z$ .

### *The Stick-Slip Energy Spikes*

The relative sharpness of the energy spikes in Figure 7 compared with the profile upon which they are superimposed makes it possible to estimate the energy barriers. While the repeat unit for hexyl shows a single spike the profile for pentyl contains two such discontinuities in each stress-slip cycle. The effect arises when, in response to the shear stress incurred by the displacement the conformation jumps fail to access the lowest-energy conformation appropriate to that particular bilayer configuration, leaving the lattice in a strained condition in a metastable state. At a subsequent bilayer displacement the additional strain imposed on the lattice is sufficient to destabilise it and to flip it into the lowest-energy conformation. The effect appears to be analogous to that observed in the stick-slip *force* discontinuities observed by Israelachvili and his coworkers in their surface-force studies [7–10] and discussed by them and by others [12].



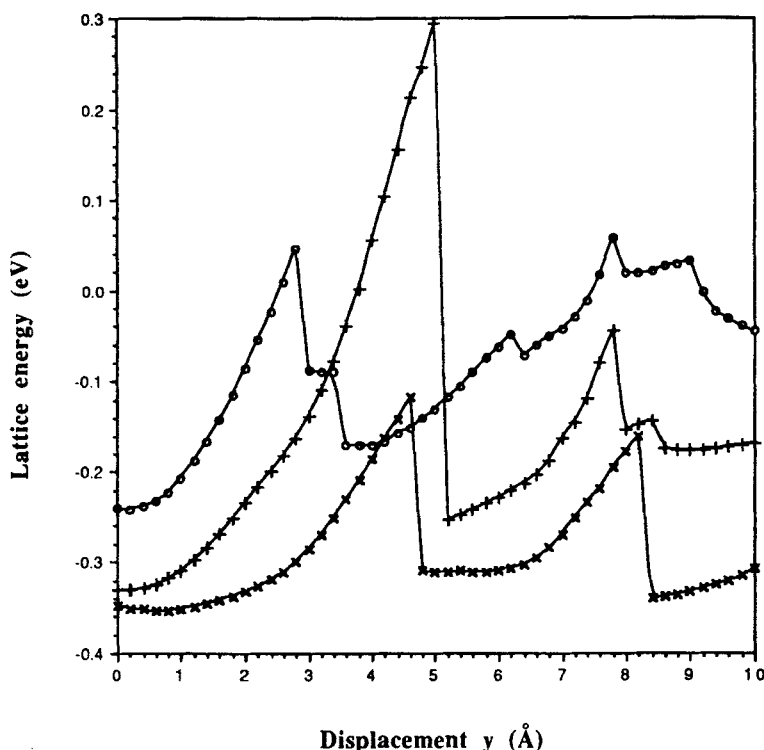


FIGURE 10 Profiles for layer displacements perpendicular to the  $a$  axis in  $C_6H_{13}$  at different values of the penetration parameter  $z = -1.0 \text{ \AA}$  ( $\circ$ -),  $-0.5 \text{ \AA}$  ( $+$ -) and  $0.0 \text{ \AA}$  ( $\times$ -). The points have been joined to distinguish the overlapping profiles more clearly.

But although the discontinuity features in Figure 7 look similar to the surface-force results it must be remembered that the systems involved differ in two important respects. The first is that in the surface-force investigations the chains lie parallel to the moving surfaces rather than normal to them as in the Y-structured Langmuir bilayers that are considered in this work. Secondly, the extents of the shear displacements in the two cases are on very different scales: the displacements of the layers in the surface-force measurements are in the range of microns, rather than the one nanometre limit that we have imposed, although the authors of the surface-force work on the thin layers remark that atomic-scale stick-slip motion may also be occurring in their systems, but that if so it is beyond their current resolution [10]. Despite the latter important distinction it is interesting that in their atomic force microscope investigation of friction on a graphite surface Mate *et al.*, found force-profile discontinuities of the stick-slip type which were

indeed on an atomic scale (0 to 20 Å) [6], and are similar to the ‘plucking’ features found in the force profiles of sliding alkane monolayers from MD simulations [16].

It was decided to investigate the stick-slip spikes by comparing their features with some of the relaxation properties found in the surface force studies of layer displacements. Israelachvili and his colleagues have described several interesting aspects of the relaxation within lubricant films [7–11] as one was subjected to a micron-scale sliding motion across the other. They found, for example, that the force profile responded to an increased velocity of the translating stage by reducing the amplitudes of the stick-slip oscillations, until at a critical velocity they were eliminated. Although the calculations conducted here do not involve a time dimension, the effect of increasing the speed of the layer displacements may to a certain extent be simulated in the ‘static mode’ by increasing the intervals at which the displacements (*e.g.*,  $x$  in Figs. 7–9) are imposed. This may be justified by the following argument. As described at the beginning of Section 4.1, at any bilayer configuration with displacement  $x_i$  the *initial* positions of the atoms (from which the relaxation begins) were chosen to be the *final* positions of the atoms after relaxation from the relaxation of configuration  $x_{i-1}$ . After the relaxation of configuration  $x_i$  the resulting atomic positions were used as a starting point to initiate the relaxation of configuration  $x_{i+1}$ . This procedure was followed at each of the displacements of the range  $0 < x < 10$  Å. Now if the  $x_{i+1} - x_i$  interval is small, this slight additional strain causes the lattice in configuration  $x_{i+1}$  to relax to a structure which is close to that of configuration  $x_i$  which is a nearby stable structure in the conformation space of the lattice. Repetition of this procedure leads to a series of conformations of progressively more delicate metastable equilibria until finally, like a house of cards, the structure collapses into a lower state. Conversely, a *larger*  $x_{i+1} - x_i$  interval would hinder the attainment of a train of metastable states near  $x_i$ , favouring instead a relaxation to a lower-energy state. In a time-mode description, this is the condition that obtains when the mutual displacement of the bilayer components is too *rapid* for the accession of those metastable states near  $x_i$ . The consequent collapse of the strained lattice to its lowest energy state would then result in the elimination of the stick-slip discontinuities, as found for lubricant layers subjected to higher displacement velocities [7–11].

Figure 11 shows a single stick-slip spike for the hexyl bilayer at  $z = 0.0$  with displacement intervals simulating increasing velocities for the motion. The result is a dramatic reduction in the amplitude of the spike as the lattice conformation at  $x_{i+1}$  finds it progressively more difficult to access the

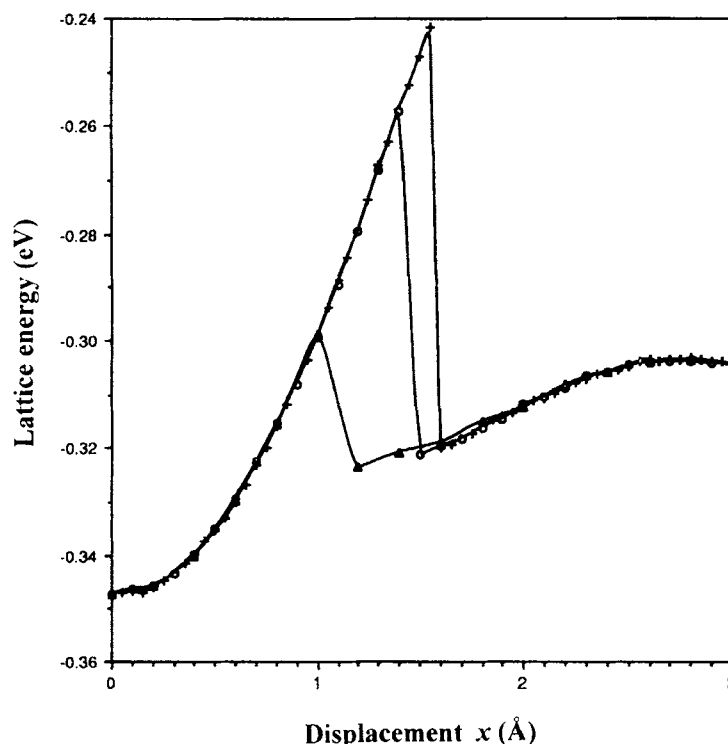


FIGURE 11 The first stick-slip energy spike for the  $C_6H_{13}$  bilayer in Figure 7 at three different displacement intervals  $\delta x = 0.2 \text{ \AA}$  ( $\Delta$ -),  $0.1 \text{ \AA}$  ( $\circ$ -) and  $0.05 \text{ \AA}$  ( $+$  -). The spike is most pronounced for small  $\delta x$ .

metastable states near  $x_i$ . The two parts of Figure 12 cast an interesting light on the nature of the stick-slip spikes by superposing different curves on to the energy profile. In part (a) the superposed curve is the number of steps taken by the simulation to achieve relaxation at each bilayer configuration. It clearly indicates that relief from the stick-slip condition is accompanied by a sharp peak denoting a sudden and substantial structural reorganisation, as the system exits the metastable region near  $x_i$  to relax to the lowest energy state. The superposed curve in part (b) is the root mean square torsion, which we use as a measure of departure of the chain conformation from all-*trans*. It shows that the metastable states associated with the stick-slip energy spikes are characterised by a steadily increasing number of non-*trans* linkages as observed experimentally in the study of strains in flexible chains in plasticised films [29]. This response to the shear forces is analagous to the results described in Section 3 above in which lateral pressures were imposed

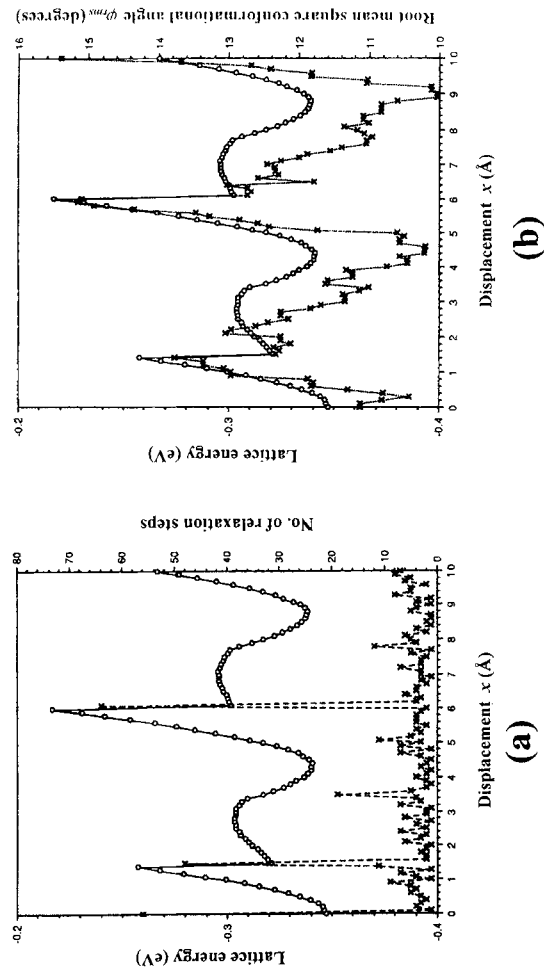


FIGURE 12 The correlation between the energy profile (—○—) and (a) the number of steps to relaxation  $N_{rel}$ (—×—) and (b) the root mean square torsional angle in the chains  $\phi_{rms}$ (—×—). The number  $N_{rel}$  is a measure of the amount of structural reorganisation required to achieve relaxation and  $\phi_{rms}$  monitors the departure of the chain system from its all-*trans* conformation.

in a monolayer so as to produce stresses greater than those obtaining in alkane lattices; we recall that the alkyl chains similarly responded by assuming non-planar chain conformations. In the present instance Figure 12(b) shows that on relaxation to the lowest energy structure for the particular  $x$  configuration, the chains jump to lower  $\varphi_{\text{rms}}$  values.

### 4.3. Quantitative Estimations: Correlation with Measurement

There are obvious differences between the idealised bilayer model used in our calculations and the contact surface that would obtain in any of the actual layer systems described in the Introduction. This should warn us that any correlation that we may find between quantities furnished by our atomistic calculations and measured values of bulk (or even molecular) properties should be treated with caution. But this should not preclude such comparisons, as they can elucidate the extent to which our models fall short of real systems.

#### *Coefficient of Friction*

The coefficient of friction may be estimated from the forces of the penetration and sliding motions. The *maximum* slopes in the energy profiles in the small-penetration region of Figures 5 and 6 ( $z$  between  $-0.5$  and  $-1.0$  Å) is about  $3 \times 10^{-10}$  N, and can be identified as the normal load, *i.e.*, the force perpendicular to the direction of motion. In order to derive bulk-like frictional parameters from an energy profile consisting of a succession of energy minima separated by barriers it must be supposed that the resistance to the motion (the frictional force) derives from the expenditure of work to surmount the energy barriers; the thermal energy thereafter released is then dissipated into the layers. From the area of the layer unit cell with  $d = 4.42$  Å this force implies a pressure of about 18 kbar ( $1.8 \times 10^9$  Pa), which is of the order of the pressures used in tribological investigations. Those appearing in normal lubricated engineering contacts are about an order of magnitude smaller, comparing with  $3 \times 10^8$  Pa in the MD simulations of alkyl-tailed surfactants [20], which in terms of the present model would imply a very small degree of interpenetration of the alkyl layers.

The force associated with the sliding motion in the bilayers expressed by Amontons' law as a fraction of the normal load defines the coefficient of friction  $\mu$ . The sliding motion is described by the various profiles that we

have discussed from their depictions in Figures 7–10. These are obviously harder to characterise by a single parameter than was the force normal to the direction of motion, but it is reasonable to suppose that the force associated with surmounting the energy barriers plays a rôle in determining the resistance to the sliding motion. If this force is evaluated from the greatest positive gradient at the energy barriers it is about  $1.4 \times 10^{-10}$  N at  $z = -0.5 \text{ \AA}$  for the hexyl chain. Combined with the normal force derived above this implies a coefficient of friction of  $\mu \approx 0.5$ .

In fact, measured values of  $\mu$  for surfaces lubricated with fatty acids of molecular weight 85–100 (which would also be those of the  $\text{C}_6\text{H}_{13}$  or  $\text{C}_7\text{H}_{15}$  chains) are indeed close to 0.5 [4], although since the profile does not have a constant gradient it could be argued that it would be fairer to regard the value of  $\mu$  derived in this way as an upper bound to the effective coefficient of friction.

### ***Shear Strength***

The shear strength,  $\tau$ , of the displaced bilayer system is defined as the frictional force per unit cofacial area and therefore has the units of pressure. Again using the *maximum slopes* of the energy profiles in Figure 9 to evaluate the effective frictional forces at various values of the penetration parameter  $z$ , Figure 13 shows how the two kinds of force in the definition of  $\tau$  vary with increasing mutual penetration of the layers. Although allowance must be made for the vagaries of stipulating a frictional force when such a force is derived from a sequence of energy barriers profiles such as those constituting the energy profiles in Figure 9, the force curves clearly show that the friction initially increases with the layer penetration  $-z$  at a rate which is less than that of the normal force, and passes through a maximum value. As a result, the coefficient of friction  $\mu$  decreases with layer penetration while the shear strength  $\tau$  increases from  $7 \times 10^8$  Pa at  $z = +0.5 \text{ \AA}$  to  $13 \times 10^8$  Pa at  $z = -0.5 \text{ \AA}$ . These  $\tau$  values compare with ones of the order of  $10^7$  Pa found by Briscoe *et al.*, in their studies of the shear properties of stearic acid and calcium stearate Langmuir-Blodgett bilayers [30] and calculated from the MD work by Glosli and McClelland for the sliding of alkyl chains [16]. Again it should not be surprising that the practice of deriving the force at a given  $z$  from the *maximum* (rather than a mean) *slope* of the energy profile has led to a range of  $\tau$  values that may be too high by one order of magnitude.

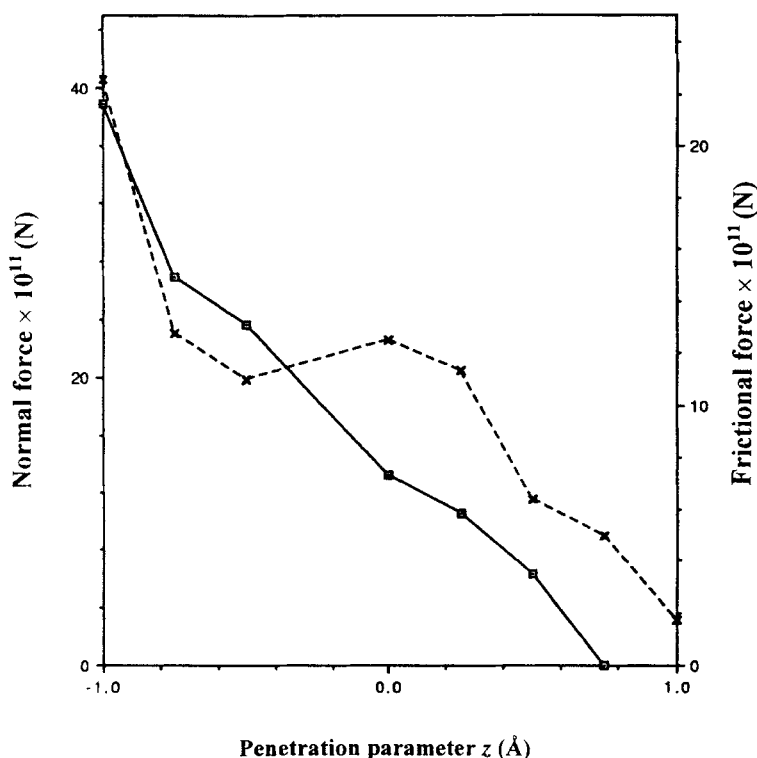


FIGURE 13 Normal ( $\square$ -) and frictional ( $\times$ -) forces in  $C_6H_{13}$  as a function of the penetration parameter  $z$ .

## 5. DISCUSSION AND CONCLUSIONS

The calculation of lattice energies by an atomistic method based on random changes in torsional angles is appropriate to lattices containing alkyl groups such as those constituting the monolayers and bilayers considered in this work. The flexibility of these chains implies the existence of a large number of energy wells in the potential energy hypersurface. After imposing such changes in the configuration of the lattice as those considered here the desired global minimum would be difficult to locate by conventional energy-minimisation techniques that are based on the curvature of the hypersurface.

It is evident that even within the fixed molecular geometry approximation, in which the bond lengths and angles are kept constant, the method provides sensible results. For example, when the lattice parameter  $d$  is in a range close

to that of an alkane lattice, the chains, in an all-*trans* conformation are predicted to be perpendicular to the surface, but when the surface pressure is reduced by increasing  $d$  the chains develop a tilt, while still largely retaining their *trans* conformations. This prediction is consistent with the Langmuir monolayer isotherms, which reveal a collapse of the substrate-normal chains at low lateral pressures [28]. It also agrees with the MD results of Tildesley and his co-workers on both monolayer [17] and bilayers [20] of dioctadecyl dimethyl ammonium chloride surfactant films: these investigations showed that increasing the molecular area (reducing the chain density of the film) leads to decreasing chain tilt angles until the chains actually lie in the substrate plane.

The results presented in Section 4.2 record the diminishing energy barriers to the mutual displacements within the bilayers as the chain length increases. Since the positions of the barriers at small penetration are constant, being governed by the periodicity of the lattice, decreasing barriers imply diminishing maximum slopes; consequently longer alkyl chains result in lower frictional forces. This is qualitatively what is found in measurements in bulk samples [4]; however the  $\mu \propto 1/n_C$  relationship between the coefficient of friction  $\mu$  and the alkyl chain length  $n_C$  that was proposed in this reference is not found here.

The bilayer motions which occur at large values of  $-z$ , the penetration parameter, correspond to high normal pressures. Since local heating effects and drastic effects on structures (molecular geometry distortions and bond ruptures) are expected to occur here, atomistic simulations of the kind described here would be of limited application. However it is useful to note (Section 4.2) that with increasing negative values of  $z$  the profile shows a damping of the energy barriers and it starts to lose its periodic character. To obtain more information than this would require that the displacement be monitored for distances needing considerably greater computing power than that employed for these calculations. However the prediction of the damping of the barriers has an important implication: it is an interesting reminder of the well-known inequality  $\mu_{\text{static}} > \mu_{\text{dynamic}}$  which the atomistic model described here would account for as follows. It was observed in the discussion of Figure 12(b) in Section 4.2 that the response of the bilayer lattice to a shear stress is the assumption of non-planar conformations of the alkyl chains. Even after relaxation from the limiting strain associated with the slip-stick spike the  $\varphi_{\text{rms}}$  values show that the alkyls are not all-*trans*. It would therefore appear that an all-*trans* conformation, which is the equilibrium structure of a lattice of alkyl chains, is not a favourable one for a shear condition. Consequently the initial barriers encountered by the



newly enmeshed layers are successively reduced as the progress of the sliding results in a partial randomisation of the chain conformations. The *trans*-to-*gauche* changes in the chains have been described in the contexts of experimental data [29] and of MD calculations on sliding in surfactant monolayers [17] and bilayers [20].

In order to attempt a correlation with experimental measurements it was necessary to extract two quantities from the calculations: the normal force, which is perpendicular to the layers, and the friction force, which is in the plane of the layer interface and in the direction of the motion. Since the energy profile consists of an approximately periodic succession of maxima and minima, the system is a non-conservative one, so that the work done on the bilayer in order to surmount an energy barrier is then presumably dissipated as heat. Since the force is thus non-uniform, it has been supposed that the friction was sensitive to the shape of the regions of the energy profile that are associated with the ascent, and not with the descent of the barriers. The practice of deriving the friction from the *maximum* positive slope of the barriers (rather than attempting to evaluate some mean value) would almost certainly be expected to lead to an overestimation of the effective frictional force characterising the sliding motion. If, as seems possible, the force is overestimated by about one order of magnitude, our calculated shear strengths  $\tau \sim 10^8$  Pa would be too high by the same factor; in this case comparison with the experimental values of  $\sim 10^7$  Pa can be considered to be fairly satisfactory.

The stick-slip spikes discussed under their topic heading in Section 4.2 are of interest as they indicate that the phenomenon investigated on a micron scale for lubricant films by Israelachvili and coworkers [7, 9–11] and on an Ångström scale for graphite by Mate *et al.* [6] also occurs in alkyl bilayers. In fact the smaller rigidity of the bilayer system compared with that of graphite implies a greater number of metastable polymorphs in the former, resulting in more pronounced discontinuities in the energy or force profiles, as suggested also by the results of MD calculations on the sliding motion of alkyl chains [16]. If this is indeed the case as implied by the calculations, then the stick-slip phenomenon is a very extensive one in nature, ranging from motions in crystalline unit cells through the squeaking of smooth sliding surfaces to geoseismic activity [9].

There still remains for investigation the effect of allowing greater randomisation on the conformational torsions in the chains, and this will require the extension of the working unit cell into a supercell and consequently considerably greater computing times. Work is in preparation to use parallel processors to study the results of reduced conformational

order on the bilayer systems and also to apply the necessary Molecular Dynamics to describe the relaxation of the strained conformations to the lowest energy state.

### Acknowledgements

The authors acknowledge helpful discussions with Dr. A. A. Torrence and are grateful to a referee who provided references to valuable work on the subject of this paper.

### References

- [1] Petty, M. C. (1996). "Langmuir-Blodgett Films", Cambridge University Press, Cambridge.
- [2] Williams, J. A. (1994). "Engineering Tribology", Clarendon Press, Oxford, pp. 350–354.
- [3] Bowden, F. P. and Tabor, D. (1994). "The Friction and Lubrication of Solids", Clarendon Press, Oxford, pp. 218–226.
- [4] Hardy, W. B. and Doubleday, I. (1922). "Boundary lubrication. The paraffin series", *Proc. R. Soc. A*, **100**, 550.
- [5] Chugg, K. J. and Chaudhri, M. M. (1993). "Boundary lubrication and shear properties of thin solid films of dioctadecyl dimethyl ammonium chloride (TA100)", *J. Phys. D: Appl. Phys.*, **26**, 1993.
- [6] Mate, C. M., McClelland, G. M., Erlandson, R. and Chiang, S. (1987). "Atomic scale friction of a tungsten tip on a graphite surface", *Phys. Rev. Lett.*, **59**, 1942.
- [7] Bhushan, B. Israelachvili, J. N. and Landman, U. (1995). "Nanotribology: friction, wear and lubrication at the atomic scale", *Nature*, **374**, 607.
- [8] Israelachvili, J. N. (1987). "Solvation forces and liquid structure as probed by direct force measurements", *Acc. Chem. Res.*, **20**, 415; Israelachvili, J. N., McGuiggan, P. M. and Homola, A. M. (1988). "Dynamic properties of molecularly thin films", *Science*, **240**, 189.
- [9] Israelachvili, J. N., McGuiggan, P. M., Gee, M. L., Homola, A. M., Robbins, M. and Thompson, P. (1990). "Liquid dynamics in molecularly thin films", *J. Phys. Condens. Matter*, **2**, SA89.
- [10] Gee, M. L., McGuiggan, P. M., Israelachvili, J. N. and Homola, A. M. (1990). "Liquid to solidlike transitions of molecularly thin films under shear", *J. Chem. Phys.*, **93**, 1895.
- [11] Yoshizawa, H. and Israelachvili, J. (1993). "Fundamental mechanisms of interfacial friction. 2. Stick-slip friction of spherical and chain molecules", *J. Phys. Chem.*, **20**, 11300.
- [12] Thompson, P. A. and Robbins, M. O. (1990). "Origin of stick-slip motion in boundary lubrication", *Science*, **250**, 792; Robbins, M. O. and Thompson, P. A. (1991). "Critical velocity of stick-slip motion", *Science*, **253**, 916.
- [13] Koike, A. and Yoneya, M. (1996). "Molecular dynamics of sliding friction of Langmuir-Blodgett monolayers", *J. Chem. Phys.*, **105**, 6060.
- [14] Xia, T. K., Ouyang, J., Ribarsky, M. W. and Landman, U. (1992). "Interfacial alkane films", *Phys. Rev. Lett.*, **69**, 1967; Vacatello, M., Yoon, D. Y. and Laskowski, B. C. (1990). "Molecular arrangements and conformations of liquid *n*-tridecane chains confined between two hard walls", *J. Chem. Phys.*, **93**, 779.
- [15] Diestler, D. J., Schoen, M. and Cushman, J. H. (1993). "On the thermodynamic stability of confined thin films under shear", *Science*, **262**, 545; Schoen, M., Diestler, D. J. and Cushman, J. H. (1993). "Shear melting of confined solid monolayer films", *Phys. Rev. B*, **47**, 5603.
- [16] Glosli, J. N. and McClelland, G. M. (1993). "Molecular dynamics study of sliding friction of ordered organic monolayers", *Phys. Rev. Lett.*, **70**, 1960.

- [17] Adolf, D. B., Tildesley, D. J., Pinches, M. R. S., Kingdon, J. B., Madden, T. and Clark, A. (1995). "Molecular dynamics simulations of dioctadecyldimethylammonium chloride monolayers", *Langmuir*, **11**, 237.
- [18] Perry, M. D. and Harrison, J. A. (1996). "Molecular dynamics studies of the frictional properties of hydrocarbon materials", *Langmuir*, **12**, 4552.
- [19] Kong, Y. C., Nicholson, D., Parsonage, N. G. and Thompson, L. (1996). "Monte Carlo simulations of a polyoxyethylene C<sub>12</sub>E<sub>2</sub> lamellar bilayer in water", *Molecular Physics*, **89**, 835.
- [20] Kong, Y. C., Tildesley, D. J. and Alejandre, J. (1997). "The molecular dynamics simulation of boundary-layer lubrication", *Molecular Physics*, **92**, 7.
- [21] Williams, D. E. (1967). "Nonbonded potential parameters derived from crystalline hydrocarbons", *J. Chem. Phys.*, **47**, 4680.
- [22] Kitaigorodsky, A. I. (1973). *Molecular Crystals and Molecules*, Academic Press, New York Chap. 9; "An atomistic simulation investigation of molecular motions in alkane chains", Loos, J. and Morton-Blake, D. A. (Student project, unpublished).
- [23] Corish, J., Morton-Blake, D. A., B  ni  re, F. and Lantoine, M., (1996). "Interaction of side-chains in poly (3-alkylthiophene) lattices", *J. Chem. Soc., Faraday Trans.*, **92**, "671.
- [24] Corish, J., Morton-Blake, D. A., B  ni  re, F., Lantoine, M. and Marchetti, M. (1996). "Atomistic simulation investigations of poly(3-alkylthiophene) lattices", *Materials Science Forum* #17, **239**, 185.
- [25] Corish, J., Feeley, D. E., Morton-Blake, D. A., B  ni  re, F., Lantoine, M. and Marchetti, M. (1997). "An atomistic investigation of chromism in a poly(3-alkylthiophene)", *J. Phys. Chem. B*, **101**, 10075.
- [26] Doucet, J., Denicolo, I. and Craievich, A. (1981). "Evidence of a phase transition in the rotator phase of the odd-numbered paraffins C<sub>23</sub>H<sub>48</sub> and C<sub>25</sub>H<sub>52</sub>", *J. Chem. Phys.*, **75**, 1523; Shih, M. C., Bohanon, T. M., Mikrut, J. M., Zschak, P. and Dutta, P. (1992). *Phys. Rev. A*, **45**, 5734; Albon, N., (1983). *J. Chem. Phys.*, **78**, 4076.
- [27] Reference 1, pp. 18–27.
- [28] Kjaer, K., Als-Nielsen, J., Helm, C. A., Tippman-Krayer, P. and M  hwald, H. (1989). "Synchrotron X-ray diffraction and reflection studies of arachidic acid monolayers at the air-water interface", *J. Phys. Chem.*, **93**, 3200.
- [29] Briscoe, B. J., Stuart, B. H. and Thomas, P. S. (1993). "Solvent induced morphological changes to polycarbonate", *Proceedings of MRS Wear Meeting*; Briscoe, B. J. and Thomas, P. S. (1994). "Structure-property relationships in thin solid poly(methylmethacrylate) boundary films", *Proceedings of the 20th Leeds–Lyon Symposium*.
- [30] Briscoe, B. J., Scruton, B. and Willis, F. R. (1973). "The shear strength of thin lubricant films", *Proc. R. Soc. A*, **333**, 99; Briscoe, B. J. and Evans, D. C. B. (1982). "The shear properties of Langmuir-Blodgett layers", *Proc. R. Soc. A*, **380**, 389.